ACS Chemical Neuroscience

pubs.acs.org/chemneuro Research Article

Multiple Actions of H_2S-Releasing Peptides in Human β-Amyloid Expressing *C. elegans*

Rafat Ali,* Rohil Hameed, Divya Chauhan, Shantanu Sen, Muhammad Wahajuddin, Aamir Nazir,* and Sandeep Verma*

Cite This: https://doi.org/10.1021/acschemneuro.2c00402 Read Online

ACCESS | Metrics & More | Article Recommendations | Supporting Information

ABSTRACT: Alzheimer's disease (AD) is a debilitating progressive neurodegenerative disorder characterized by the loss of cognitive function. A major challenge in treating this ailment fully is its multifactorial nature, as it is associated with effects like deposition of Aβ plaques, oxidative distress, inflammation of neuronal cells, and low levels of the neurotransmitter acetylcholine (ACh). In the present work, we demonstrate the design, synthesis, and biological activity of peptide conjugates by coupling a H_2S-releasing moiety to the peptides known for their Aβ antiaggregating properties. These conjugates release H_2S in a slow and sustained manner, due to the formation of self-assembled structures and delivered a significant amount of H_2S within *Caenorhabditis elegans*. These conjugates are shown to target multiple factors responsible for the progression of AD: notably, we observed reduction in oxidative distress, inhibition of Aβ aggregation, and significantly increased ACh levels in the *C. elegans* model expressing human Aβ.

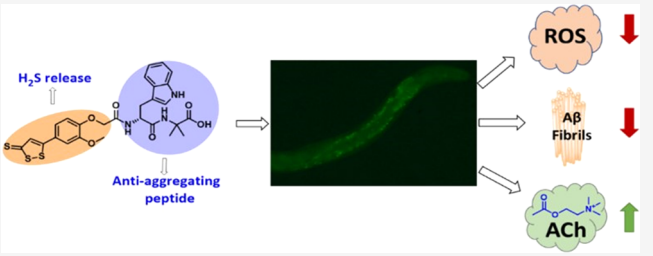

KEYWORDS: *Alzheimer's disease, Aβ aggregation, hydrogen sulfide, oxidative distress, acetylcholine, peptides*

1. INTRODUCTION

Neurodegenerative disorders, including Alzheimer's disease (AD), Parkinson's disease (PD), and Huntington's disease, affect millions of people across the globe. These ailments result in the loss of nerve cells in the central and peripheral nervous systems, thus altering critical bodily functions. AD is a common progressive neurodegenerative disease and is one of the most prevailing causes of dementia.[1] Impairment in cognitive functions, loss of memory, and the inability of body parts to carry out their normal function are some of the characteristic symptoms of AD. Although the full etiology of AD remains to be completely unraveled, the formation of Aβ senile plaques[2,3] and Tau neurofibrillary tangles,[4] degeneration of cholinergic neurons,[5] increase in oxidative distress,[6] and inflammation[7] are considered to be important factors responsible for the progression and pathophysiology of AD.

Currently available therapies for AD rely on neurotransmitter regulators and fall under two broad categories such as acetylcholinesterase inhibitors and antagonists of the *N*-methyl-D-aspartic acid receptor.[8] The problem associated with the available therapeutic approaches is that they treat only AD symptoms. On considering the pervasive devastation of AD and an acute need of managing AD patients, aducanumab—a human monoclonal antibody targeting Aβ amyloid plaque—was recently approved by US-FDA under its Accelerated Approval Program. It is also considered the first drug that addresses the underlying biology of AD.[9] Although aducanumab decreases the amount of amyloid plaques, clear evidence that it restores lost memories or cognitive function remains unanswered. Therefore, there is an urgent need to develop new strategies to target multiple aspects of AD, which can act upon disease-causing pathways instead of merely providing temporary symptomatic relief.

Hydrogen sulfide (H_2S) is an endogenous signaling gaseous molecule produced mainly by three enzymes, namely, cystathionine γ-lyase (CSE), cystathionine β-synthase (CBS), and 3-mercaptopyruvate sulfurtransferase (MPST), in different tissues.[10] Initially, there were concerns about the toxicity of H_2S gas, but it is now recognized for its antioxidant, neuroprotectant, and neuromodulator properties.[11] H_2S demonstrates these properties only when there is an optimal concentration of H_2S present in the cells, as both excessive and lower amounts of H_2S are known to have deleterious effects on biological systems.[12] H_2S is also shown to increase glutathione levels, which are otherwise depleted due to oxidative distress under disease conditions. This aspect of H_2S is primarily responsible for its neuroprotective activity.[13] Moreover, the reactive oxygen species (ROS) scavenging capacity of H_2S also contributes to its neuroprotective effects.[14] Intracellular H_2S

Received: July 13, 2022
Accepted: October 28, 2022

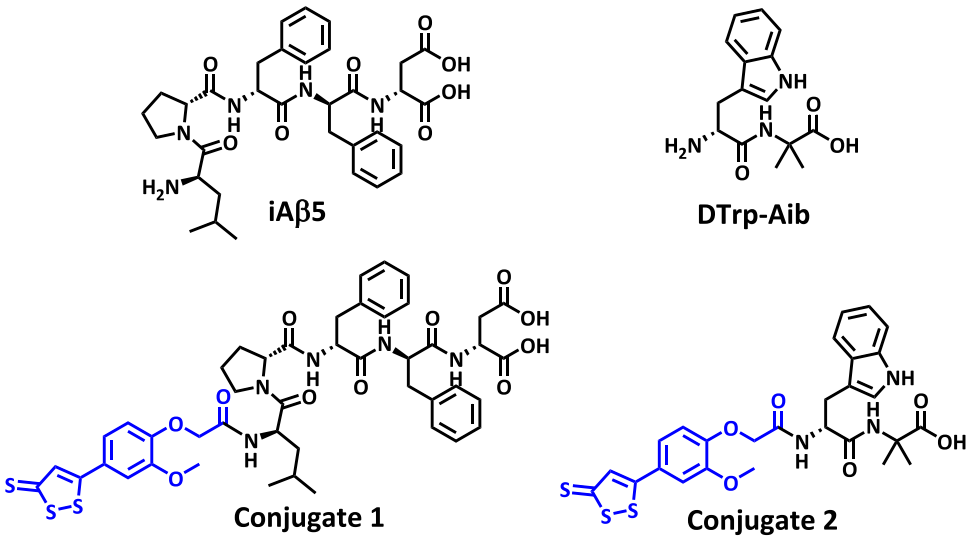

Figure 1. Chemical structure of peptides and their H_2S-releasing counterparts.

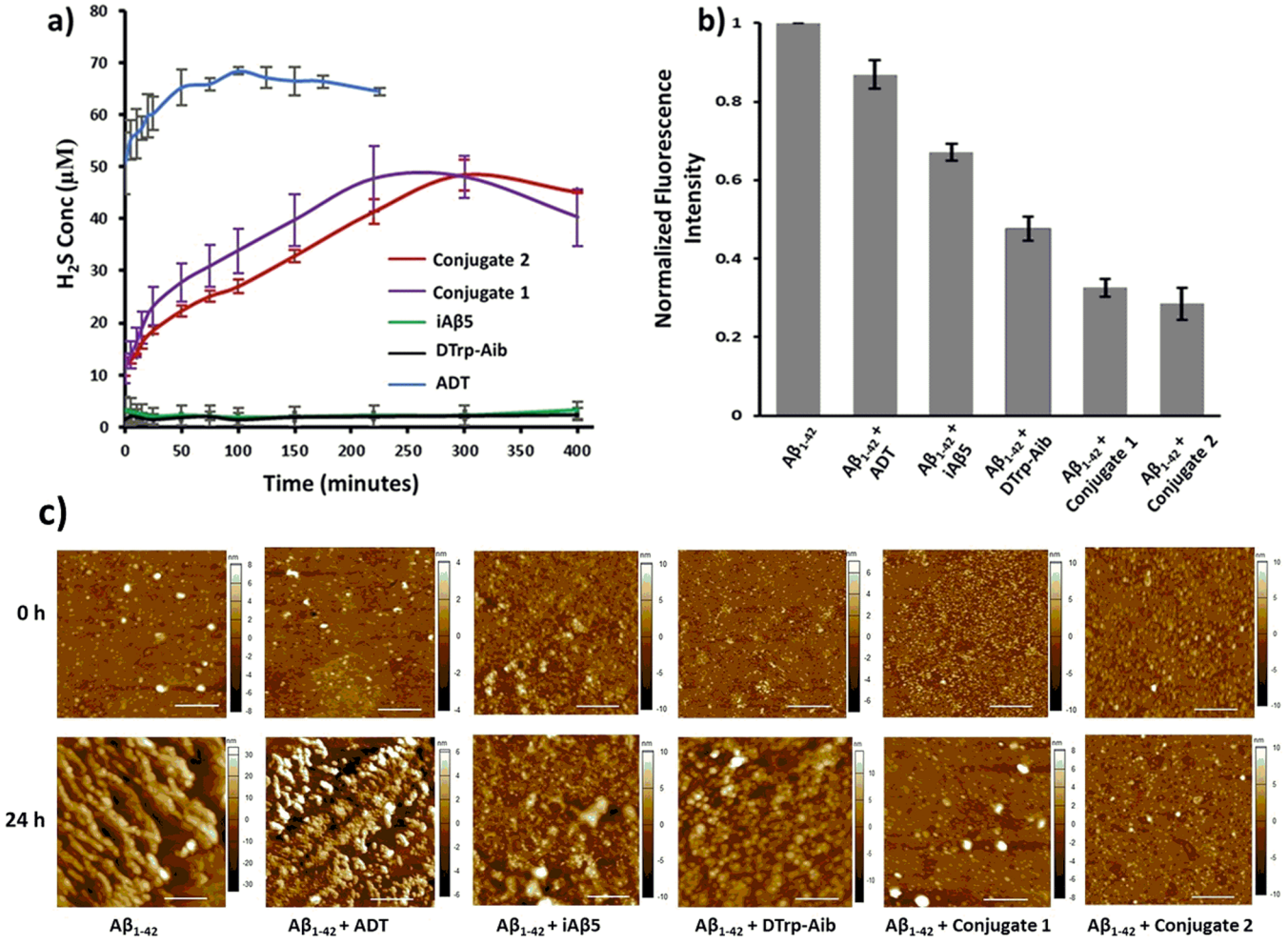

Figure 2. (a) H_2S releasing kinetics of peptide conjugates (100 μM) on coincubation with TCEP (1 mM) at 37 °C; (b) ThT assay showing Aβ_{1-42} (10 μM) aggregation and their inhibition by peptide conjugates (10 μM) on 24 h incubation at 37 °C. Each bar represents ± SD of three independent experiments; (c) AFM images of incubated Aβ_{1-42} alone and in the presence of peptide conjugates at 37 °C after 0 and 24 h time intervals. Scale bar = 500 nm.

levels as well as associated enzymes responsible for its production were found to be severely decreased in the brain samples of AD patients, leading to the decline of cognitive functions.[15] Thus, plasma H_2S levels could serve as a biomarker for diagnosis and intervention of AD.[16] Notably, several studies have also suggested a crucial role of H_2S in

https://doi.org/10.1021/acschemneuro.2c00402
ACS Chem. Neurosci. XXXX, XXX, XXX−XXX

slowing down AD progression and in manifesting therapeutic potential for its treatment.[17−21]

As discussed, the optimum level of hydrogen sulfide can reverse the pathophysiological consequences of AD. Also, the peptides that inhibit the aggregation of Aβ_{1-42} or dissolve amyloid plaques could prevent the neurotoxicity associated with Aβ oligomers/fibrils and are considered potential tools in AD therapeutics.[22] Herein, we have designed and synthesized conjugates in which we amalgamated anti-amyloidogenic peptides with a H_2S-releasing moiety. For the present study, we have selected two peptide fragments, pentapeptide iAβ5 (Leu−Pro−Phe−Phe−Asp) and dipeptide DTrp-−Aib, which are known for their β-sheet breaking and antiaggregating properties[23,24] whereas 2-(2-methoxy-4-(5-thioxo-5H-1,2-dithiol-3-yl)phenoxy)acetic acid (aryldithiolethione, ADT) were selected as the H_2S-releasing moiety, which can also inhibit dopamine-metabolizing enzyme monoamine oxidase-B (MAO-B) to offer neuroprotective properties.[25] By combining the hydrogen sulfide-releasing moiety with the peptides iAβ5 and DTrp−Aib, conjugates **1** and **2** were prepared, respectively (Figure 1). Furthermore, their effects were studied on the multiple factors associated with the progression of AD.

2. RESULTS AND DISCUSSION

2.1. Synthesis of Peptide Conjugates. The H_2S-releasing aryldithiolethione (ADT) was prepared from eugenol by following the reported protocol (Scheme S1a).[26] Initially, phenyl ether and methyl-2-(4-allyl-2-methoxyphenoxy) acetate were synthesized by the reaction of eugenol with methyl bromoacetate under alkaline conditions. The allyl group of phenyl ether on reacting with elemental sulfur at 220 °C resulted in the formation of a dithiolethione ring, which, on the subsequent acid hydrolysis of methyl ester, gave the desired aryldithiolethione. The peptides (iAβ5 and DTrp−Aib) and their H_2S-releasing conjugates (conjugate **1** and **2**) were prepared by following the standard solid-phase method of peptide synthesis using 2-chlorotrityl chloride (CTC) resin as a solid support (Scheme S1b).

2.2. Self-Assembly of Peptide Conjugates. The synthesized peptides were studied for their self-assembling tendency in aqueous solution by scanning electron microscopy (SEM), atomic force microscopy (AFM), and dynamic light scattering (DLS) measurement. The peptides iAβ5 and DTrp−Aib are unable to form any self-assembled structures in aqueous medium (Figure S4). *N*-Terminal capping of peptides with hydrophobic moieties is known to enhance their self-assembling tendency in aqueous environments and further directs their formation into distinct nanostructures.[27−29] The controlled release of therapeutic gaseous molecules has also been manifested through such self-assembled nanostructures.[26,30] Thus, peptide conjugates **1** and **2** were synthesized by conjugating the H_2S-releasing moiety at the *N*-terminal of the iAβ5 and DTrp−Aib peptides, respectively. The self-assembling properties of these conjugates were studied by SEM, AFM, and dynamic light scattering measurement data, and it was observed that these conjugates self-assembled as uniform nanospheres in aqueous medium (Figures S4−S7).

2.3. In Vitro H_2S Release Kinetics and Inhibition of Aβ_{1-42} Aggregation by Peptide Conjugates. We evaluated the hydrogen sulfide release kinetics of these conjugates by coincubating them with tris(2-carboxyethyl) phosphine (TCEP). Although the exact mechanism by which TCEP releases H_2S is not fully elucidated, it is suggested that being the strong reducing agent, TCEP initiates the H_2S release by reducing the disulfide bond of the dithiolethione group in aqueous solution.[31] The concentration of released H_2S was measured using the methylene blue assay by following the reported protocols.[32] ADT released hydrogen sulfide almost instantaneously on coincubating with TCEP and reached the maximum release in ∼100 min. Conjugate **1** released H_2S slowly and achieved the maximum concentration at ∼250 min, whereas conjugate **2** also released H_2S in a slower manner to achieve the maximum release at ∼350 min (Figure 2a). Such slow-releasing phenomena of these peptide conjugates could be attributed to the self-assembled structures adopted by these conjugates.

These peptide conjugates were then evaluated for their ability to inhibit aggregation of the Aβ_{1-42} peptide by the well-established thioflavin T (ThT) assay.[33] Both iAβ5 and DTrp−Aib are known β-sheet breaker peptides involved in disrupting amyloidogenic driving forces, either hindering the early association of toxic amyloid intermediates or disassembling the preformed fibrils. We assessed whether these peptides retain their antiaggregating properties on conjugation with the aryldithiolethione moiety. We observed that the newly synthesized aryldithiolethione-conjugated peptides **1** and **2** significantly inhibit the fibrillation of the Aβ_{1-42} peptide (Figure 2b). To further confirm the antiaggregating properties of synthesized peptide conjugates, morphological changes in the Aβ_{1-42} peptide during incubation were studied by AFM imaging (Figure 2c). AFM images demonstrate that Aβ_{1-42} alone will form fibrillating structures after 24 h of incubation, whereas no significant fibrillar or higher order aggregating structures were observed when Aβ_{1-42} was coincubated with conjugates **1** and **2**. With this, we have achieved the synthesis of the peptide conjugates, which release hydrogen sulfide in a controlled manner as well as inhibit the aggregation of the Aβ_{1-42} peptide.

2.4. H_2S Release by Peptide Conjugates Inside *Caenorhabditis elegans*. H_2S is produced endogenously in mammalian cells and its optimum physiological concentration is crucial for performing various biological processes.[34] The physiological importance of H_2S is very well studied in a nematode worm, *C. elegans*. For example, H_2S proved to be valuable for *C. elegans* longevity by restricting aging through controlling cellular stress pathways.[35−37] Moreover, targeted H_2S delivery to mitochondria has also been found to improve the neuromuscular health of *C. elegans*.[38] The beneficial role of peptide-mediated H_2S delivery in transgenic *C. elegans* was also recently reported.[26]

Herein, we have used a wild-type N2 strain of *C. elegans* as an in vivo system to evaluate the efficient delivery of H_2S by designed peptide conjugates within a whole organismal environment. Under physiological conditions, H_2S release from aryldithiolethiones is mainly catalyzed by cytochrome P450-dependent monooxygenase in the presence of NADPH and dioxygen.[39] Mechanistic studies revealed that aryldithiolethione finally converted to H_2S and para-methoxy-acetophenone through the formation of aryldithiolone and dithiolium cation intermediates. *C. elegans* has cytochrome P450 genes as well as NADPH/$NADP^+$ machinery, thus providing suitable conditions required for H_2S release from these conjugates.[40,41] The H_2S-sensing fluorescent probe 7-azido-4-methylcoumarin (AzMC) was used for studying the ability of these conjugates to deliver H_2S inside the worm body.[35,42] An increase in the fluorescence intensity of AzMC can directly be correlated with

https://doi.org/10.1021/acschemneuro.2c00402
ACS Chem. Neurosci. XXXX, XXX, XXX−XXX

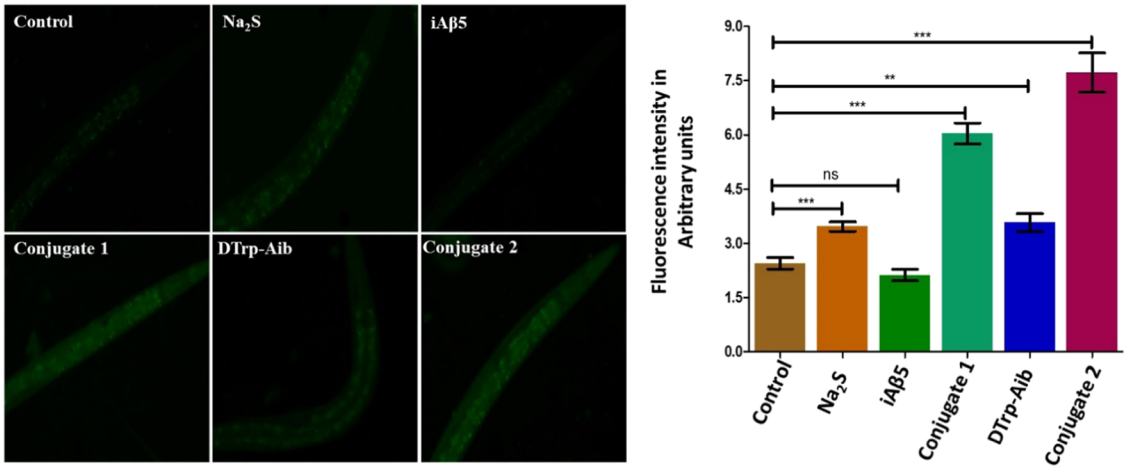

Figure 3. Fluorescent micrographs of the *C. elegans* N2 strain (wild type) showing the delivery of H_2S inside the worm as detected via the AzMC dye by the peptide conjugates (1 mM) and H_2S quantification by normalizing fluorescence intensity. The number of worms in each set is 30, and observations were measured in triplicate (***$P < 0.05$).

the amount of H_2S released inside the worm. The transparent body of *C. elegans* makes it an ideal tool for live cell imaging in such experimental settings (Figure 3). The delivery of a relative amount of hydrogen sulfide inside *C. elegans* was quantified by normalizing the fluorescence intensity of AzMC. A significant increase in fluorescence intensity was observed in *C. elegans* worms treated with peptide conjugates **1** and **2** compared to control and sodium sulfide (Na_2S)-treated worms, suggesting the importance of such peptide frameworks in H_2S delivery (Figure 3).

2.5. Peptide Conjugates Reduce Oxidative Distress in *C. elegans*. Oxidative distress is considered to be one of the major driving forces behind almost all neurodegenerative disorders including AD.[43] A high level of reactive oxygen species (ROS) creates an imbalance in redox signaling and further imparts irreversible damage to diverse cellular biomolecules. Protein carbonylation, lipid peroxidation, nucleobase hydroxylation, DNA double-stranded breaks (DSBs), etc., are considered to be some of the deleterious effects associated with such oxidative damages due to the increased level of ROS production.[44−48] Ultimately, ROS upregulation leads to cellular necrosis or apoptosis and further impairment of different body parts including the central nervous system.[49] Thus, quenching oxidative burden is extremely desirable for treating such neurodegenerative ailments. For studying the effect of these conjugates on the ROS level, we employed the wild-type N2 strain of *C. elegans*, as it enables quantification of ROS levels within the in vivo system.[50] Hydrogen peroxide was used to increase the ROS levels in *C. elegans*, and the 2′,7′-dichlorodihydrofluorescein diacetate (H_2DCFDA) assay was used for estimating the ROS level as per the earlier reported protocol.[51] Among all compounds, peptide conjugate **2** was found to be the most effective one, which significantly lowered ROS levels in wild-type *C. elegans* (Figure 4), whereas peptide conjugate **1** reduced the ROS load to a moderate extent but not as effective as conjugate **2**.

We have also measured the lipofuscin accumulation and reduced glutathione (GSH) levels in the wild-type N2 strain of *C. elegans* for further evaluating the antioxidant potential of peptide conjugates **1** and **2**. Lipofuscin is an autofluorescent pigment formed when lipid peroxidation products (like

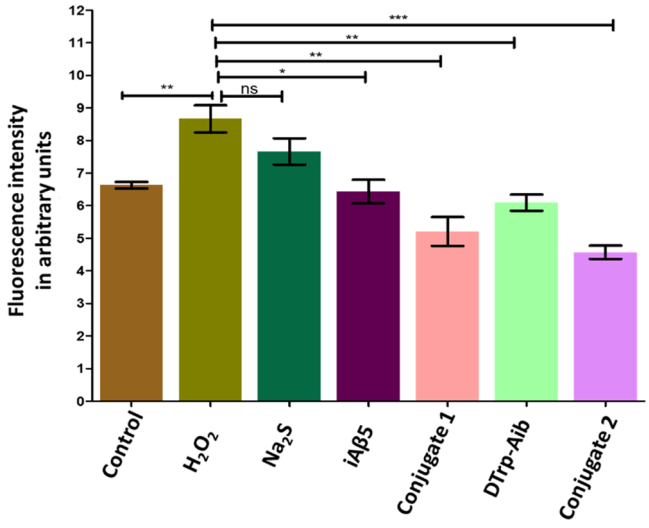

Figure 4. ROS estimation using the DCFDA assay in the N2 strain of *C. elegans* (wild type) upon the treatment of peptide conjugates (1 mM) in the presence of H_2O_2 (positive control at 20 mM). The number of worms in each set is 100, and observations were measured in triplicate (***$P < 0.05$).

reactive aldehydes, lipid radicals, etc.) react with proteins, lipids, and other vulnerable groups. Accumulation of lipofuscin serves as an important marker of oxidative damage.[52] Similarly, the level of GSH also serves as an important marker of oxidative distress, and an increase in GSH levels upon treatment of the molecules can directly be correlated to its antioxidant properties.[53] The lipofuscin accumulation is measured by observing its autofluorescence, and GSH levels are estimated through HPLC analysis in wild-type *C. elegans*. We observed a significant reduction in the accumulation of lipofuscin pigment and increased GSH levels in *C. elegans* treated with peptide conjugates compared to untreated ones (Figures S8 and S9). These results indicate that these peptide conjugates significantly reduce oxidative distress in *C. elegans* and possess convincing antioxidant properties.

2.6. Peptide Conjugates Reduce $A\beta_{1-42}$ Amyloid Deposit in Transgenic *C. elegans*. Deposition of soluble neurotoxic $A\beta$ oligomers was considered the main culprit

https://doi.org/10.1021/acschemneuro.2c00402
ACS Chem. Neurosci. XXXX, XXX, XXX−XXX

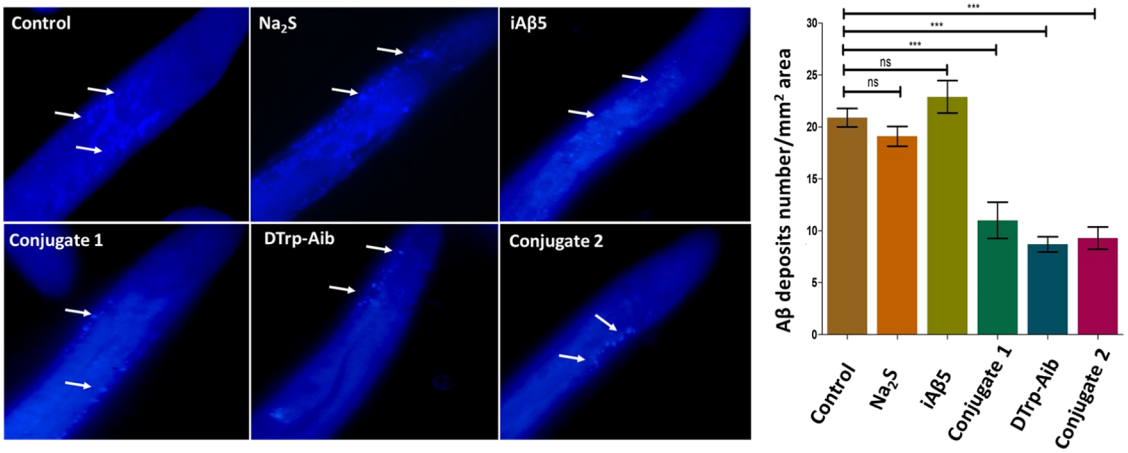

Figure 5. Fluorescent microscopic images of the transgenic *C. elegans* CL2006 strain (expressing human Aβ_{1-42} protein), showing the deposition of Aβ aggregates upon treatment of peptide conjugates (1 mM) and their quantification. The number of worms in each set is 30, and observations were measured in triplicate (***$P < 0.05$).

responsible for the initiation of AD pathogenesis. These Aβ oligomers further polymerize and accumulate as senile amyloid plaques in the brain, which worsen the conditions of AD patients.[54] Preventing the formation of fatal Aβ aggregates or dissolution of already generated amyloid plaques is considered one of the most effective strategies applied for the development of AD therapies.[55−57] Thereafter, we assessed the role of the test peptides in preventing the formation of Aβ aggregates in the CL2006 strain of *C. elegans*. CL2006 is a transgenic strain that expresses human Aβ_{1-42} in its muscle. This strain enables screening of potential compounds, as it exhibits a paralysis phenotype when there are increased aggregation conditions, and the reversal of paralysis is observed when a potential antiaggregating intervention reduces such aggregation.[58,59] The extent of amyloid β expression can also be visualized and quantified by employing the fluorescent dye thioflavin S.[60] Thioflavin S binds specifically to amyloid fibrils and not with Aβ monomers, resulting in precise staining of amyloid aggregates in vivo. The quantification of Aβ fibrils was carried out by employing transgenic *C. elegans* strain CL2006 after staining with thioflavin S, making it amenable to visualize and quantify Aβ deposits in *C. elegans*. All of the peptides except iAβ5 were found to be effective in reducing the accumulation of Aβ_{1-42} aggregate loads in transgenic *C. elegans* compared to the untreated population (Figure 5). These results indicate that the synthesized peptide conjugates significantly inhibit the aggregation of Aβ_{1-42}, thus resulting in reduced amyloid deposits in *C. elegans*.

2.7. Peptide Conjugates Significantly Increase the ACh Levels of Transgenic *C. elegans*. Another most important factor responsible for AD progression is degeneration of cholinergic neurons, resulting in a low level of acetylcholine (ACh) production in AD patients.[61] Acetylcholine is an important neurotransmitter involved in both central and peripheral nervous systems and plays a pivotal role in cognitive functions. To study the effect of our compounds on ACh levels, we employed the transgenic CL2006 strain of *C. elegans*. This transgenic strain expresses human Aβ_{1-42}, is reported to have significantly lower levels of ACh compared to wild-type *C. elegans*, and therefore serves as a perfect in vivo model system for studying AD pathogenesis.[62]

The transgenic CL2006 strain of *C. elegans* was treated with the synthesized compounds, and after 48 h of treatment, the neurotransmitter acetylcholine was quantified using LC/MS-MS. Our synthesized H_2S-releasing peptide conjugates significantly increased the ACh levels in transgenic worms (Figure 6). Moreover, the treatment of these peptide

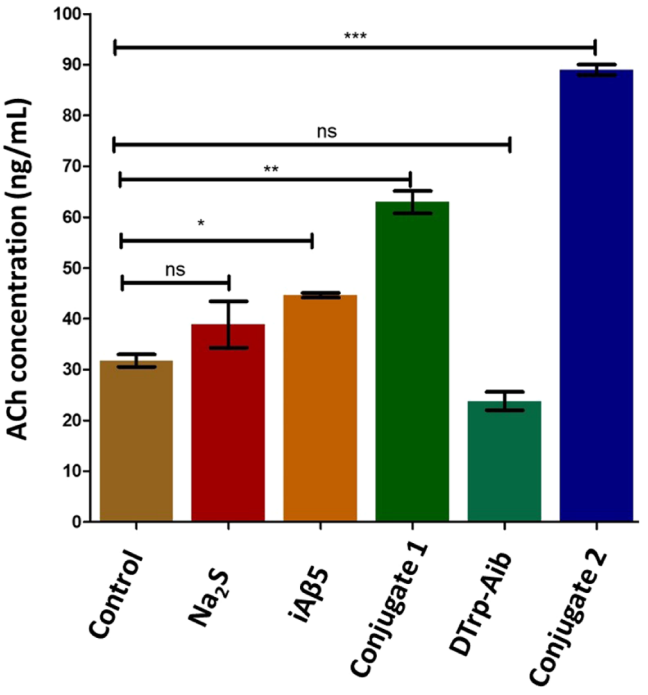

Figure 6. Estimation of acetylcholine (ACh) levels in the transgenic CL2006 strain of *C. elegans* (expressing human Aβ_{1-42} peptide) upon the treatment of peptide conjugates (1 mM) via LC/MS-MS. The number of worms in each set is 3000, and observations were measured in triplicate (***$P < 0.05$).

conjugates lowered the activity of acetylcholinesterase (AChE), an enzyme responsible mainly for the degradation of ACh (Figure S11). An increase in ROS and the formation of toxic Aβ oligomers/fibrils are mainly considered to be responsible for low levels of ACh in AD. Oxidative distress initiates the degeneration of the cholinergic system, particularly by inducing lipid peroxidation of the neuronal membrane,[63] whereas Aβ amyloid impairs the cholinergic system by

https://doi.org/10.1021/acschemneuro.2c00402
ACS Chem. Neurosci. XXXX, XXX, XXX−XXX

modulating muscarinic receptor signaling, choline acetyltransferase (ChAT) activity, reduction of choline uptake, which eventually result in the depleted level of ACh.[64−66] Among all, peptide conjugate **2** proved to be the most effective one in increasing the ACh levels of worms (Figure 6). Peptide conjugate **2** has better hydrogen sulfide-releasing kinetics, improved ROS scavenging property, and significant $A\beta_{1-42}$ aggregation inhibitory profile and displays good inhibition of AChE activity. The synergistic effect of all these properties is responsible for the considerable increase of the ACh level by conjugate **2** in transgenic worms.

3. CONCLUSIONS

In summary, we present data on the design and synthesis of a new class of hydrogen sulfide-releasing antiaggregating peptides whose self-assembling tendency in the solution results in slow H_2S release. The peptide conjugates exhibit significant antioxidant properties and are also able to reduce Aβ aggregate burden in *C. elegans*. Moreover, H_2S-donating peptide conjugate **2** significantly increases the ACh level, which is an important neurotransmitter playing a crucial role in memory, as well as the learning process, in the transgenic *C. elegans* model expressing human amyloid β. This newly developed class of peptide conjugates ameliorates the multiple factors associated with AD and may play a beneficial role in the development of new therapeutics for this debilitating ailment.

4. MATERIALS AND METHODS

4.1. General Information. TLC (thin-layer chromatography) silica gel $60F_{254}$ plates (Merck, Darmstadt, Germany) were used to monitor the progress of the reaction by visualizing it with UV light at 254 nm. The peptide $A\beta_{1-42}$ was obtained from Invitrogen (cat. no. 03-111). For chromatographic separation, 100−200 mesh silica gel was used. ^{1}H NMR spectra were acquired on a JEOL-JNM spectrometer operating at either 400 or 500 MHz frequency at 25 °C with 2−10 mM compound concentrations in suitable solvents using tetramethyl silane (TMS) as the internal standard or the solvent signals as secondary standards. The chemical shifts (δ) were displayed in ppm scales. The multiplicities of NMR signals were assigned as s (singlet), d (doublet), t (triplet), q (quadruplet), br (broad), dd (doublet of doublet), and m (multiplet or unresolved lines). Spectra of ^{13}C NMR were recorded at either 100 or 125 MHz frequency. On an Agilent mass spectrometer, HRMS spectra were acquired. At 25 °C, UV−vis absorption spectra were obtained with a Varian CARY 100 Bio UV−vis spectrophotometer equipped with a 10 mm quartz cell. The fluorescence of ThT was determined by a SpectraMax iD3 Multi-Mode Microplate Reader.

4.2. Procedure for Fmoc Protection of D-Tryptophan and 2-Aminoisobutyric Acid. D-Tryptophan or aminoisobutyric acid (Aib, 19.39 mmol) was dissolved in a 10% Na_2CO_3 (aq)/dioxane (60 mL, 1:1) mixture at 0 °C. After 10 min of stirring, the solution of Fmoc−OSu (19.39 mmol) in dioxane (20 mL) was added dropwise to the reaction mixture by maintaining the reaction temperature at 0 °C. The reaction mixture was then allowed to stir overnight at room temperature. After that, dioxane was evaporated, and the aqueous layer was acidified to pH 3 using 6 N HCl. The aqueous layer was washed with ethyl acetate (two times), and after that, combined organic layers were washed with brine and dried over sodium sulfate. Ethyl acetate was evaporated under reduced pressure to give the desired Fmoc-protected amino acids as solid powders, which were used directly for the next reaction without purification. Yield (for Fmoc−DTrp−OH, 8.2 g, 19.23 mmol, 99%; for Fmoc−Aib−OH, 5.3 g, 16.29 mmol, 84%).

4.3. Synthesis of 2-(2-Methoxy-4-(5-thioxo-5H-1,2-dithiol-3-yl)phenoxy)acetic Acid. This was prepared by following the reported procedure.[26] A brown-colored solid; ^{1}H NMR (400 MHz, DMSO-d_6): δ/ppm = 7.87 (s, 1H), 7.68−7.29 (m, 2H), 6.98 (d, J = 8.4 Hz, 1H), 4.80 (s, 2H), 3.88 (s, 3H); ^{13}C NMR (100 MHz, DMSO-d_6): δ/ppm = 215.37, 174.47, 170.22, 151.37, 149.70, 135.17, 124.83, 120.84, 113.62, 111.13, 65.27, 56.47; FTIR (KBr) 3557, 3471, 3073, 2932, 1752, 1524, 1477, 1274, 1152, 1019, 950, 769, 632; ESI-HRMS: $[M - H]^-$, calculated for $C_{12}H_9O_4S_3^-$ = 312.9668, observed = 312.9669.

4.4. Synthesis of (R)-2-(2-Amino-3-(1H-indol-3-yl)-propanamido)-2-methylpropanoic Acid (DTrp−Aib). *4.4.1. Preparation of (R)-2-(2-Amino-3-(1H-indol-3-yl)-propanamido)-2-methylpropanoic Acid−Resin.* The reaction vessel was charged with 152 mg (0.2 mmol) of 2-chlorotrityl chloride (CTC) resin containing 1.32 mmol/g of substitution. The resin was swollen in dichloromethane (DCM, 3 mL) for 30 min. After swelling, the resin was washed with dry DCM. A solution of Fmoc−Aib−OH (195 mg, 0.6 mmol) and *N*,*N*-diisopropylethylamine (DIPEA, 209 μL, 1.2 mmol) in dry DCM/DMF (1:1 ratio, 6 mL) was then added to the reaction vessel. The reaction mixture was allowed to agitate for 3 h by nitrogen gas purging. After that, HPLC-grade methanol (1 mL) was added to the reaction mixture to mask any reactive group on the resin. After 15 min, solvents were filtered, and the resin was washed subsequently with DMF and DCM. The resin was then treated with a 20% piperidine/DMF solution (3 mL), agitated for 5 min, and filtered. The resin was treated once more with the 20% piperidine/DMF solution (5 mL), purged with nitrogen gas for 25 min, and then filtered. The resin was then rinsed with DMF. To this resin, a solution of Fmoc−DTrp−OH (256 mg, 0.6 mmol) and hydroxybenzotriazole (HOBt, 81 mg, 0.6 mmol) in DMF (4 mL) was added, and the reaction mixture was agitated by nitrogen gas purging. This was followed by the addition of *N*,*N*′-diisopropylcarbodiimide (DIC, 94 μL, 0.6 mmol), and the reaction mixture allowed further 3 h agitation under nitrogen gas purging. The Kaiser test was used to check the coupling of amino acids. If the test was positive, the stirring process would continue until the Kaiser test was negative. Following completion of the coupling, the resin was filtered and washed with DMF. After thorough washing, the resin was treated with the 20% piperidine/DMF solution (3 mL), agitated for 5 min, and filtered. The resin was treated once more with the 20% piperidine/DMF (5 mL) solution, agitated for additional 25 min by nitrogen gas purging, and then filtered. The resin was rinsed with DMF and finally with DCM. After proper washing, the resin was then vacuum-dried.

4.4.2. Preparation of (R)-2-(2-Amino-3-(1H-indol-3-yl)-propanamido)-2-methylpropanoic Acid. The aforementioned resin was then treated with 10 mL of a mixture of trifluoroethanol/acetic acid/DCM (10:10:80%) and stirred for 1 h. The resin was removed by filtration followed by solvent evaporation below 45 °C under decreased pressure. Diethyl ether was used to precipitate the dipeptide. The precipitate was then filtered and rinsed with diethyl ether. The precipitate was finally dried under vacuum to yield the crude peptide (70 mg). The crude peptide was purified by reversed-phase HPLC (RP-HPLC) using 0.1% trifluoroacetic acid (TFA) in a water/acetonitrile solvent system with a C-18 column, and then the pure sample was lyophilized to yield DTrp−Aib as a white powder. Yield (52 mg, 0.18 mmol, 89.8%). ESI-HRMS $(M + H)^+$ calculated for $C_{15}H_{20}N_3O_3^+$ = 290.1499; observed = 290.1498.

4.5. Synthesis of iAβ5. *4.5.1. Preparation of Leu−Pro−Phe−Phe−Asp(OtBu)−Resin.* It was prepared by following the same procedure used for the synthesis of DTrp−Aib using 2-chlorotrityl chloride resin (0.2 mmol) as a solid support with Fmoc−Asp(OtBu)−OH, Fmoc−Phe−OH, Fmoc−Pro−OH, and Fmoc−Leu−OH as Fmoc-protected amino acids.

4.5.2. Preparation of Leu−Pro−Phe−Phe−Asp (iAβ5). The Leu−Pro−Phe−Phe−Asp(OtBu)−resin was treated with 10 mL of a mixture of trifluoroacetic acid/triisopropylsilane/H_2O/DCM (30:2.5:2.5:65%), and the reaction mixture was allowed to be stirred for 2 h. The resin was filtered, and the solvents of the filtrate were evaporated under low pressure below 45 °C. Diethyl ether was used to precipitate the peptide. The crude peptide (115 mg) was obtained by drying the precipitate under vacuum. The crude peptide was purified using RP-HPLC with 0.1% TFA in a water/acetonitrile solvent system and a C-18 column. The purified sample was then

https://doi.org/10.1021/acschemneuro.2c00402
ACS Chem. Neurosci. XXXX, XXX, XXX−XXX

lyophilized to obtain the peptide in the form of a white powder. Yield (90 mg, 0.14 mmol, 70.5%). ESI-HRMS $(M + H)^+$ calculated for $C_{33}H_{44}N_5O_8^+$ = 638.3184; observed = 638.3200.

4.6. Synthesis of Conjugate 1. The solution of 2-(2-Methoxy-4-(5-thioxo-5H-1,2-dithiol-3-yl)phenoxy)acetic acid (188.6 mg, 0.6 mmol) and HOBt (81 mg, 0.6 mmol) in DMF (4 mL) was added to the Leu−Pro−Phe−Phe−Asp(OtBu)−resin (0.2 mmol). To this solution, DIC (94 μL, 0.6 mmol) was added and the reaction mixture was allowed to be stirred for 4 h by nitrogen gas purging. The Kaiser test was used to check the coupling of a compound to the resin. After the reaction was done, the resin was washed with DMF and finally with DCM. The properly washed resin was kept in vacuum for further drying. The dried resin was added to 10 mL of a solution of TFA/triisopropylsilane/H_2O/DCM (30:2.5:2.5:65%) and allowed to be stirred for 2 h. The resin was filtered, and then the solvents of the filtrate were evaporated under low pressure below 45°C. Diethyl ether was used to precipitate the peptides. The precipitate was further dried under vacuum to give the crude peptide (150 mg). The crude peptide was purified using RP-HPLC with 0.1% TFA in water/acetonitrile and a C-18 column. The purified sample was then lyophilized to obtain the orange-yellow powder of conjugate **1**. Yield (117 mg, 0.12 mmol, 63%) ^{1}H NMR (500 MHz, DMSO-d_6) δ (ppm) = 8.29 (d, J = 7.5 Hz, 1H), 8.14 (d, J = 8.2 Hz, 1H), 8.00 (d, J = 8.3 Hz, 1H), 7.84 (s, 1H), 7.75 (d, J = 8.0 Hz, 1H), 7.44−7.38 (m, 2H), 7.26−7.08 (m, 10H), 6.97 (d, J = 9.1 Hz, 1H), 4.62 (s, 2H), 4.69−4.41 (m, 3H), 4.42−4.32 (m, 1H), 4.32−4.22 (m, 1H), 3.84 (s, 3H), 3.59−3.51 (m, 1H), 3.42−3.34 (m, 1H), 3.00−2.85 (m, 2H), 2.81−2.72 (m,2H), 2.70−2.49 (m, 2H), 1.95−1.65 (m, 4H), 1.65−1.46 (m, 1H), 1.47−1.29 (m, 2H), 0.83 (d, J = 6.5 Hz, 6H); ^{13}C NMR (125 MHz, DMSO-d_6) δ (ppm) = 220.16, 179.10, 177.45, 176.91, 176.36, 176.01, 175.80, 175.43, 172.18, 156.25, 154.71, 142.82, 140.03, 134.53, 133.28, 133.24, 131.52, 131.43, 129.97, 125.58, 119.24, 115.93, 72.55, 64.53, 61.33, 59.07, 58.76, 53.92, 53.66, 51.95, 45.60, 42.92, 42.51, 41.26, 34.00, 29.57, 29.35, 28.50, 26.65. ESI-HRMS $(M - H)^-$ calculated for $C_{45}H_{50}N_5O_{11}S_3^-$ = 932.2674; observed = 932.2657.

4.7. Synthesis of Conjugate 2. The solution of 2-(2-methoxy-4-(5-thioxo-5H-1,2-dithiol-3-yl)phenoxy)acetic acid (188.6 mg, 0.6 mmol) and HOBt (81 mg, 0.6 mmol) in DMF (4 mL) was added to the DTrp−Aib−resin (0.2 mmol). To this solution, DIC (94 μL, 0.6 mmol) was added and the reaction mixture was agitated for 4 h by nitrogen gas purging. The Kaiser test was used to evaluate a sample of resin to monitor the coupling. After completion of coupling, the resin was rinsed with DMF and finally with DCM. After drying the resin under vacuum, the resin was then treated with 10 mL of trifluoroethanol/acetic acid/DCM (10:10:80%), which was agitated for 1 h. The resin was filtered, and the solvents of the filtrate were evaporated at reduced pressure and below 45 °C temperature. Diethyl ether was used to precipitate the peptide. The resulting precipitate was filtered and vacuum-dried to produce the crude peptide (117 mg). The crude peptide was purified using RP-HPLC with 0.1% TFA in water/acetonitrile and a C-18 column. The purified sample was then lyophilized to obtain the orange-yellow powder of conjugate **2**. Yield (95 mg, 0.16 mmol, 81%). ^{1}H NMR (400 MHz, DMSO-d_6) δ 12.20 (s, 1H), 10.82 (s, 1H), 8.28 (s, 1H), 8.03 (d, J = 8.5 Hz, 1H), 7.81 (s, 1H), 7.58 (d, J = 7.9 Hz, 1H), 7.34-7.29 (m, 2H), 7.16 (dd, J = 8.4, 2.1 Hz, 1H), 7.10 (d, J = 2.1 Hz, 1H), 7.02 (t, J = 7.6 Hz, 1H), 6.91 (t, J = 7.3 Hz, 1H), 4.76−4.57 (m, 1H), 4.54−4.45 (m, 2H), 3.80 (s, 3H), 3.12−3.06 (m, 1H), 2.97−2.79 (m, 1H), 1.32 (s, 3H), 1.29 (s, 3H). ^{13}C NMR (125 MHz, DMSO-d_6) δ 215.36, 175.91, 174.39, 170.89, 167.08, 151.37, 149.78, 136.55, 135.20, 127.95, 125.01, 124.37, 121.36, 120.74, 119.04, 118.71, 114.10, 111.74, 111.04, 110.12, 67.79, 56.49, 55.50, 53.07, 28.75, 25.46, 25.25. ESI-HRMS $(M - H)^-$ calculated for $C_{27}H_{26}N_3O_6S_3^-$ = 584.0989, observed = 584.0983.

4.8. Synthesis of 7-Azido-4-methylcoumarin (AzMC). It was prepared from 7-amino-4-methylcoumarin by following the procedure reported in the literature.[67]

4.9. High-Performance Liquid Chromatography (HPLC) Analysis. HPLC analysis was done with an Agilent technologies 1260 infinity system equipped with a quaternary pump (G1311B), an auto liquid sampler (G1329B), a diode array detector (G1315D), and an analytical scale-fraction collector (G1364C). A ZORBAX Eclipse plus C-18 (250 × 4.6 mm^2) column with a particle size of 5 μm was used for peptide purification. The solvent flow rate was 1.0 mL/min, and the mobile phase was made up of solvent A (0.1% TFA in Milli-Q water) and solvent B (0.1% TFA in acetonitrile).

4.10. Scanning Electron Microscopy (SEM). Field emission scanning electron microscopy (FESEM) images were taken with an FEI QUANTA 200 microscope operated at 10 kV. From freshly made 1 mM solutions of peptides in water (for iAβ5 and DTrp−Aib), 10% methanol/water (for conjugate **2**), or 50% methanol/water (for conjugate **1**), 15 μL were drop-casted on copper stubs and left to dry at room temperature overnight. The samples were then dried under high vacuum for additional 15 min. After gold coating for 45 s, FESEM images were taken.

4.11. Atomic Force Microscopy (AFM). From the stock solution of peptides (0.1 mM in 10% MeOH/water for conjugate **1** and 0.1 mM in 1% MeOH/water for conjugate **2**), 15 μL was drop-casted onto the surface of a silicon wafer at room temperature. The samples were left to dry at room temperature overnight, and then they were dried under high vacuum for additional 30 min before they were scanned. An atomic force microscope (Asylum Research, Oxford Instruments, MFP-3D Origin) was used to scan the samples at room temperature. The tapping mode and a constant force of 21 N/m were used to do the scanning. A cantilever from NANOSENSORS with the following features was used: material: n$^+$-silicon, resistivity: 0.01−0.02 Ω cm, resonance frequency: 146−236 kHz, thickness: 7.1 μm, length: 225 μm, width: 38 μm, and force constant: 21−98 N/m.

4.12. Dynamic Light Scattering (DLS). The DLS measurement of a 0.1 mM peptide solution (for conjugate **1**: 10% methanol/water and for conjugate **2**: 1% methanol/water were used) was carried out using a NanoBrook 90Plus PALS particle sizer and a ζ-potential analyzer from Brookhaven Instrument. HPLC-grade methanol and Milli-Q water were used for sample preparation. The diameter of the particle was computed using a standard equation incorporating the dynamic viscosity of the appropriate solvent, which is integrated into Brookhaven Instrument software.

4.13. H_2S Release Kinetics. Tetrahydrofuran was used to make 40 mM stock solutions of peptide conjugates **1** and **2**. To start the reactions, 75 μL from the 40 mM stock solutions of peptide conjugates was added to 30 mL of phosphate buffer (pH 7.4) containing 1.0 mM TCEP (an accelerator for H_2S release). In this way, the final working concentration of 100 μM for conjugates was achieved. This reaction mixture was incubated at 37 °C. Aliquots of 1.0 mL from the reaction mixture were taken at regular time intervals and mixed into a methylene blue cocktail: 30 mM $FeCl_3$ in 1.2 M HCl (200 μL), 20 mM *N*,*N*-dimethyl-1,4-phenylenediamine sulfate in 7.2 M HCl (200 μL), and 1% w/v $Zn(OAc)_2$ in water (100 μL). After 15 min, a UV−vis spectrophotometer was used to measure the solution's absorbance at 670 nm. Following the reported protocol, the H_2S concentration was calculated by converting absorbance readings to H_2S concentrations using the standard Na_2S concentration−absorbance calibration curve.[32] All experiments were repeated thrice.

4.14. Thioflavin T Assay. Lyophilized Aβ_{1-42} were dissolved in 1,1,1,3,3,3-hexafluoro-2-propanol (HFIP) to maintain the monomer state of Aβ_{1-42} and then aliquoted to different vials according to the desired concentration. HFIP of the aliquoted samples was removed under gentle nitrogen flow and was then kept for additional 30 min in a vacuum desiccator for the complete removal of HFIP traces. The residual Aβ_{1-42} peptide was then dissolved in a minimum amount of 2 mM NaOH (aq). The Aβ_{1-42} peptide solution was sonicated for 30 s (three times) in cold water. The Aβ_{1-42} peptide was diluted with 1× PBS buffer of pH 7.4 to the final concentration of 40 μM; 50 μL from this Aβ_{1-42} solution (40 μM) was taken and immediately added to the 50 μM ThT solution in 1× PBS buffer with and without an inhibitor in a 96-well plate in such a way that the final concentration of Aβ_{1-42} and peptide conjugates in the solution was 10 μM. The plate was then incubated for 24 h at 37 °C and ThT fluorescence was then measured by setting the excitation wavelength at 435 nm and the emission wavelength at 485 nm.

https://doi.org/10.1021/acschemneuro.2c00402
ACS Chem. Neurosci. XXXX, XXX, XXX−XXX

4.15. Atomic Force Microscopy (AFM) Imaging for Studying $A\beta_{1-42}$ Aggregation. The $A\beta_{1-42}$ solution was prepared in 1× PBS with or without peptide conjugates in such a way that the final concentration of $A\beta_{1-42}$ and peptide conjugates in the solution was 10 μM. The samples were then allowed for incubation at 37 °C. From these solutions, 50 μL of samples were taken at 0 and 24 h time intervals and diluted four times with Milli-Q water. From the diluted samples, 5 μL was drop-casted on a glass slide. After drying at room temperature for 3−4 h, the samples were washed with Milli-Q water (three times). Before AFM scanning, the samples were dried at room temperature for 12 h, followed by 30 min of final drying under high vacuum. The samples were scanned with AFM (Asylum Research, Oxford Instruments, MFP-3D Origin) under tapping mode. A cantilever with the following features was used: (1) supplier: NANOSENSORS, material: n^+-silicon, resistivity: 0.01−0.02 Ω cm, resonance frequency: 146−236 kHz, thickness: 7.1 μm, length: 225 μm, width: 38 μm, force constant: 21−98 N/m, and (2) supplier: Asylum Research probe, OXFORD instrument, material: silicon, resonance frequency: 50−90 kHz, force constant: 0.6−3.5 N/m.

4.16. H_2S Measurement in *C. elegans*. The measurement of H_2S was carried out as per the standard method.[35] The nematodes were raised on standard NGM medium streaked with bacteria E. coli (OP50). Prior to the experiment, respective adult nematodes were incubated at 20 °C for 2 h with a fluorescent H_2S sensor, 7-azido-4-methylcoumarin (AzMC, 50 μM). *C. elegans* were treated with respective compounds (1 mM) from the L1 stage to the young adult stage. Images of adult nematodes were obtained at the young adult stage with a Carl Zeiss fluorescence microscope at 10× using an FITC filter. The semiquantitative measurement of fluorescence intensity in the unit area was then obtained using ImageJ software as described previously.[68]

4.17. Estimation of Reactive Oxygen Species (ROS) in *C. elegans*. The estimation of reactive oxygen species (ROS) levels upon the treatment of compounds was carried out in the N2 strain (wild type) by the 2′,7′-dichlorodihydrofluorescein diacetate (H_2-DCFDA) assay.[26] In brief, the H_2-DCFDA dye diffused inside the worm body cells, and host cell esterase cleaved diacetate by which H_2-DCFDA was converted into 2′,7′-dichlorodihydrofluorescein (H_2-DCF) and was finally oxidized into 2′,7′-dichlorofluorescein (DCF) by host cell ROS. The emitted fluorescence was measured at λ_{ex} of 495 nm and λ_{em} at 512−527 nm. As a positive control for the experiment, we treated the young adult worms of respective groups with H_2O_2 (20 mM, Sigma cat: 32 338-1) and incubated them for 1 h at 22 °C followed by washing thrice with 1× PBS. For analysis, 100 worms were transferred into a 96-well plate. 100 μL of the H_2-DCFDA dye (100 μM) was added to each well, and fluorescence was measured at λ_{ex} of 495 nm and λ_{em} at 512−527 nm. The respective compounds were treated to worms from the L1 stage to the young adult stage. The fluorescence was measured immediately before and after the addition of dye and after incubation of 1 h. The data analysis was done by subtracting the initial to 0 h fluorescence and then to the final fluorescence reading, which was then divided by 100 to calculate the fluorescence intensity per worm.

4.18. Quantification of $A\beta_{1-42}$ Aggregates in *C. elegans*. The quantification of $A\beta$ fibrils was carried out employing the transgenic *C. elegans* strain CL2006 (dvIs2 [pCL12(unc-54/human Abeta peptide 1−42 minigene) + rol-6(su1006)]) expressing amyloid β, which, when stained by thioflavin S, makes it amenable to visualize and quantify the aggregation pattern.[62] The worms were treated from the L1 stage to the young adult stage with respective compounds (1 mM). The young adult worms of the CL2006 strain were washed thrice with M9 buffer, followed by fixation with 4% paraformaldehyde incubated at 4 °C overnight. The fixed worms were freeze-fractured using liquid nitrogen to disrupt the tough worm cuticle, thus making worm bodies permeable for the thioflavin S dye. The freeze-fractured *C. elegans* were treated with permeabilization solution (300 μL; 125 mM Tris, pH 7.4, 5% fresh β-mercaptoethanol, and 1% Triton X-100) and incubated at 37 °C for 48 h. Finally, worms were washed with PBST (0.1%) followed by thioflavin S staining solution (Sigma, 0.125% concentration) treatment for 2 min prepared in 50% ethanol. The stained worms were washed with 50% ethanol and mounted on glass slides in 50% glycerol. The images were acquired by a Carl Zeiss fluorescence microscope at 40× objective and analyzed by ImageJ.

4.19. Quantification of the Acetylcholine Level of *C. elegans* Using LC-MS/MS. *4.19.1. Instrument Conditions.* Acetylcholine in *C. elegans* was analyzed by an LC-MS/MS (ABSciex 4000, Toronto, Canada) equipped with an API electrospray ionization (ESI) source by following the reported protocol.[69] The curtain gas, auxiliary gas, and collision gas parameters of the instrument were set, respectively, to 30, 35, and 30. The voltage for the ion spray was set to 5500 V. The parameters for the compounds: entrance potential (EP), declustering potential (DP), collision energy (CE), and collision exit potential (CXP), each of which, respectively, was 10, 135, 12, and 30 V. Zero air was used as the source gas, and nitrogen was used as both collision and curtain gas. The mass spectrometer was set to the ESI positive ion mode, and the ions were found by the multiple reaction monitoring (MRM) mode for monitoring the transition of m/z 146.20 precursor ion $[M + H]^+$ to m/z 87.10 for acetylcholine. The separation was done with a Phenomenex Luna HILIC (3 μm, 150 × 4.6 mm^2) column and a mobile phase of acidified acetonitrile (0.1% formic acid): Milli-Q water (0.1% formic acid) in the ratio of 90:10 (v/v) at a flow rate of 0.5 mL/min. Analyst software version 1.4.1 was used for data acquisition and analyses (Applied Biosystems, MDS Sciex Toronto, Canada).

4.19.2. Sample Preparation. Acetylcholine was taken out of lysate from 3000 worms using a simple protein-precipitation method, like what was described before with a few small changes. In short, 150 μL of cold acetonitrile was added to 50 μL of cell lysate as an extracting solvent. The mixture was then vortexed for another 10 min and centrifuged at 10 000 rpm for another 10 min. The supernatant was separated and injected into a column to be analyzed with LC-MS/MS.

■ ASSOCIATED CONTENT

Supporting Information

The Supporting Information is available free of charge at https://pubs.acs.org/doi/10.1021/acschemneuro.2c00402.

Synthetic schemes; HPLC chromatograms; scanning electron microscopy (SEM); atomic force microscopy (AFM); dynamic light scattering (DLS) measurement; and copies of ^1H NMR, ^{13}C NMR, and mass spectra (PDF)

■ AUTHOR INFORMATION

Corresponding Authors

Rafat Ali − *Department of Chemistry, Indian Institute of Technology Kanpur, Kanpur 208016 Uttar Pradesh, India;* orcid.org/0000-0002-1737-0257; Email: rafatali@iitk.ac.in

Aamir Nazir − *Division of Neuroscience and Ageing Biology, CSIR-Central Drug Research Institute, Lucknow 226031, India; Academy of Scientific and Innovative Research (AcSIR), Ghaziabad 201002, India*; Email: anazir@cdri.res.in

Sandeep Verma − *Department of Chemistry, Indian Institute of Technology Kanpur, Kanpur 208016 Uttar Pradesh, India; Centre for Nanoscience and Mehta Family Center for Engineering in Medicine, Indian Institute of Technology Kanpur, Kanpur 208016 Uttar Pradesh, India;* orcid.org/0000-0002-2478-8109; Email: sverma@iitk.ac.in

Authors

Rohil Hameed − *Division of Neuroscience and Ageing Biology, CSIR-Central Drug Research Institute, Lucknow 226031, India; Academy of Scientific and Innovative Research (AcSIR), Ghaziabad 201002, India*

Divya Chauhan − *Academy of Scientific and Innovative Research (AcSIR), Ghaziabad 201002, India; Division of Pharmaceutics & Pharmacokinetics, CSIR-Central Drug Research Institute, Lucknow 226031, India*

Shantanu Sen − *Department of Chemistry, Indian Institute of Technology Kanpur, Kanpur 208016 Uttar Pradesh, India;* orcid.org/0000-0001-7363-3907

Muhammad Wahajuddin − *Academy of Scientific and Innovative Research (AcSIR), Ghaziabad 201002, India; Division of Pharmaceutics & Pharmacokinetics, CSIR-Central Drug Research Institute, Lucknow 226031, India;* Present Address: Institute of Cancer Therapeutics, School of Pharmacy and Medical Sciences, Faculty of Life Sciences, University of Bradford, Richmond Road, Bradford BD7 1DP, United Kingdom

Complete contact information is available at: https://pubs.acs.org/10.1021/acschemneuro.2c00402

Author Contributions

S.V. designed, conceptualized, and supervised the study. R.A. contributed to designing the study, conceptualization, synthesis, and biophysical experiments. A.N. and R.H. designed and performed *C. elegans* model, expressing human Aβ, experiments. D.C. and M.W. contributed to LC-MS experiments concerning ACh quantifications. S.S. performed ThT assays. All authors contributed to writing the manuscript.

Notes

The authors declare no competing financial interest.

■ ACKNOWLEDGMENTS

S.V. thank JC Bose National Fellowship (SERB) for generous research funding. R.A. thanks DST for Inspire research grant and fellowship [DST/INSPIRE/04/2019/002454]. R.H. thanks CSIR, India, for a predoctoral fellowship and AcSIR for doctoral registration. S.S. thanks MHRD for a predoctoral fellowship. The authors acknowledge Swati Chaturvedi for helping in the LC/MS experiment. Nematode strains used in this work were provided by the C. elegans Genetics Centre (CGC), University of Minnesota, MN, USA, which is funded by the US National Institutes of Health National Center for Research Resources (NIH-NCRR). CSIR-CDRI Communication No. 10485.

■ REFERENCES

(1) Alzheimer's Association. 2018 Alzheimer's Disease Facts and Figures. *Alzheimer's Dement.* **2018**, *14*, 367−429.
(2) Hardy, J.; Allsop, D. Amyloid Deposition as the Central Event in the Aetiology of Alzheimer's Disease. *Trends Pharmacol. Sci.* **1991**, *12*, 383−388.
(3) Selkoe, D. J. The Molecular Pathology of Alzheimer's Disease. *Neuron* **1991**, *6*, 487−498.
(4) Frost, B.; Jacks, R. L.; Diamond, M. I. Propagation of Tau Misfolding from the Outside to the inside of a Cell. *J. Biol. Chem.* **2009**, *284*, 12845−12852.
(5) Davies, P.; Maloney, A. J. F. Selective loss of central cholinergic neurons in Alzheimer's disease. *Lancet* **1976**, *308*, 1403.
(6) Butterfield, D. A.; Halliwell, B. Oxidative Stress, Dysfunctional Glucose Metabolism and Alzheimer Disease. *Nat. Rev. Neurosci.* **2019**, *20*, 148−160.
(7) McGeer, P. L.; Rogers, J. Anti-inflammatory Agents as a Therapeutic Approach to Alzheimer's Disease. *Neurology* **1992**, *42*, 447−449.
(8) Cummings, J. L.; Morstorf, T.; Zhong, K. Alzheimer's Disease Drug-Development Pipelines: Few Candidates, Frequent Failures. *Alzheimers Res. Ther.* **2014**, *6*, 37.
(9) U.S. Food and Drug Administration (FDA). FDA Grants Accelerated Approval for Alzheimer's Drug. https//www.fda.gov/drugs/postmarket-drug-safety-information-patients-and-providers/aducanumab-marketed-aduhelm-information (accessed June 7, 2021).
(10) Kimura, H. Production and Physiological Effects of Hydrogen Sulfide. *Antioxid. Redox Signal.* **2014**, *20*, 783−793.
(11) Kumar, M.; Sandhir, R. Hydrogen Sulfide in Physiological and Pathological Mechanisms in Brain. *CNS Neurol. Disord. Drug Targets* **2018**, *17*, 654−670.
(12) Paul, B. D.; Snyder, S. H.; Kashfi, K. Effects of Hydrogen Sulfide on Mitochondrial Function and Cellular Bioenergetics. *Redox Biol.* **2021**, *38*, No. 101772.
(13) Kimura, Y.; Kimura, H. Hydrogen Sulfide Protects Neurons from Oxidative Stress. *FASEB J.* **2004**, *18*, 1165−1167.
(14) Whiteman, M.; Armstrong, J. S.; Chu, S. H.; Jia-Ling, S.; Wong, B. S.; Cheung, N. S.; Halliwell, B.; Moore, P. K. The Novel Neuromodulator Hydrogen Sulfide: An Endogenous Peroxynitrite "Scavenger"? *J. Neurochem.* **2004**, *90*, 765−768.
(15) Eto, K.; Asada, T.; Arima, K.; Makifuchi, T.; Kimura, H. Brain Hydrogen Sulfide Is Severely Decreased in Alzheimer's Disease. *Biochem. Biophys. Res. Commun.* **2002**, *293*, 1485−1488.
(16) Disbrow, E.; Stokes, K. Y.; Ledbetter, C.; Patterson, J.; Kelley, R.; Pardue, S.; Reekes, T.; Larmeu, L.; Batra, V.; Yuan, S.; Cvek, U.; Trutschl, M.; Kilgore, P.; Alexander, J. S.; Kevil, C. G. Plasma Hydrogen Sulfide: A Biomarker of Alzheimer's Disease and Related Dementias. *Alzheimer's Dement.* **2021**, *17*, 1391−1402.
(17) Wei, H.-J.; Li, X.; Tang, X. Therapeutic Benefits of H 2 S in Alzheimer' s Disease. *J. Clin. Neurosci.* **2014**, *21*, 1665−1669.
(18) Giuliani, D.; Ottani, A.; Zaffe, D.; Galantucci, M.; Strinati, F.; Lodi, R.; Guarini, S. Hydrogen Sulfide Slows down Progression of Experimental Alzheimer's Disease by Targeting Multiple Pathophysiological Mechanisms. *Neurobiol. Learn. Mem.* **2013**, *104*, 82−91.
(19) Giovinazzo, D.; Bursac, B.; Sbodio, J. I.; Nalluru, S.; Vignane, T.; Snowman, A. M.; Albacarys, L. M.; Sedlak, T. W.; Torregrossa, R.; Whiteman, M.; Filipovic, M. R.; Snyder, S. H.; Paul, B. D. Hydrogen Sulfide Is Neuroprotective in Alzheimer's Disease by Sulfhydrating GSK3β and Inhibiting Tau Hyperphosphorylation. *Proc. Natl. Acad. Sci. U.S.A.* **2021**, *118*, No. e2017225118.
(20) Cheng, X. J.; Gu, J. X.; Pang, Y. P.; Liu, J.; Xu, T.; Li, X. R.; Hua, Y. Z.; Newell, K. A.; Huang, X. F.; Yu, Y.; Liu, Y. Tacrine-Hydrogen Sulfide Donor Hybrid Ameliorates Cognitive Impairment in the Aluminum Chloride Mouse Model of Alzheimer's Disease. *ACS Chem. Neurosci.* **2019**, *10*, 3500−3509.
(21) Aboulhoda, B. E.; Rashed, L. A.; Ahmed, H.; Obaya, E. M. M.; Ibrahim, W.; Alkafass, M. A. L.; Abd El-Aal, S. A.; ShamsEldeen, A. M. Hydrogen Sulfide and Mesenchymal Stem Cells-Extracted Microvesicles Attenuate LPS-Induced Alzheimer's Disease. *J. Cell. Physiol.* **2021**, *236*, 5994−6010.
(22) Goyal, D.; Shuaib, S.; Mann, S.; Goyal, B. Rationally Designed Peptides and Peptidomimetics as Inhibitors of Amyloid-β (Aβ) Aggregation: Potential Therapeutics of Alzheimer's Disease. *ACS Comb. Sci.* **2017**, *19*, 55−80.
(23) Claudio, S.; Sigurdsson, E. M.; Morelli, L.; Kumar, R. A.; Castaño, E. M.; Frangione, B. Beta-Sheet Breaker Peptides Inhibit Fibrillogenesis in a Rat Brain Model of Amyloidosis: Implications for Alzheimer's Therapy. *Nat. Med.* **1998**, *4*, 822−826.
(24) Frydman-Marom, A.; Rechter, M.; Shefler, I.; Bram, Y.; Shalev, D. E.; Gazit, E. Cognitive-Performance Recovery of Alzheimer's Disease Model Mice by Modulation of Early Soluble Amyloidal Assemblies. *Angew. Chem.* **2009**, *121*, 2015−2020.
(25) Drukarch, B.; Flier, J.; Jongenelen, C. A. M.; Andringa, G.; Schoffelmeer, A. N. M. The Antioxidant Anethole Dithiolethione Inhibits Monoamine Oxidase-B but Not Monoamine Oxidase A Activity in Extracts of Cultured Astrocytes. *J. Neural Transm.* **2006**, *113*, 593−598.

(26) Ali, R.; Pal, H. A.; Hameed, R.; Nazir, A.; Verma, S. Controlled Release of Hydrogen Sulfide Significantly Reduces ROS Stress and Increases Dopamine Levels in Transgenic: C. Elegans. *Chem. Commun.* **2019**, *55*, 10142−10145.
(27) Tao, K.; Levin, A.; Adler-Abramovich, L.; Gazit, E. Fmoc-Modified Amino Acids and Short Peptides: Simple Bio-Inspired Building Blocks for the Fabrication of Functional Materials. *Chem. Soc. Rev.* **2016**, *45*, 3935−3953.
(28) Arnon, Z. A.; Pinotsi, D.; Schmidt, M.; Gilead, S.; Guterman, T.; Sadhanala, A.; Ahmad, S.; Levin, A.; Walther, P.; Kaminski, C. F.; Fändrich, M.; Kaminski Schierle, G. S.; Adler-Abramovich, L.; Shimon, L. J. W.; Gazit, E. Opal-like Multicolor Appearance of Self-Assembled Photonic Array. *ACS Appl. Mater. Interfaces* **2018**, *10*, 20783−20789.
(29) Wiernik, G.; Mishra, N. K.; Mondal, S.; Ali, R.; Gazit, E.; Verma, S. A Colored Hydrophobic Peptide Film Based on Self-Assembled Two-Fold Topology. *J. Colloid Interface Sci.* **2021**, *594*, 326−333.
(30) Pal, H. A.; Mohapatra, S.; Gupta, V.; Ghosh, S.; Verma, S. Self-Assembling Soft Structures for Intracellular NO Release and Promotion of Neurite Outgrowth. *Chem. Sci.* **2017**, *8*, 6171−6175.
(31) Hasegawa, U.; Van Der Vlies, A. J. Design and Synthesis of Polymeric Hydrogen Sulfide Donors. *Bioconjugate Chem.* **2014**, *25*, 1290−1300.
(32) Li, M.; Li, J.; Zhang, T.; Zhao, Q.; Cheng, J.; Liu, B.; Wang, Z.; Zhao, L.; Wang, C. Syntheses, Toxicities and Anti-Inflammation of H2S-Donors Based on Non-Steroidal Anti-Inflammatory Drugs. *Eur. J. Med. Chem.* **2017**, *138*, 51−65.
(33) Xue, C.; Lin, T. Y.; Chang, D.; Guo, Z. Thioflavin T as an Amyloid Dye: Fibril Quantification, Optimal Concentration and Effect on Aggregation. *R. Soc. Open Sci.* **2017**, *4*, No. 160696.
(34) Wang, R. Physiological Implications of Hydrogen Sulfide: A Whiff Exploration That Blossomed. *Physiol. Rev.* **2012**, *92*, 791−896.
(35) Ng, L. T.; Ng, L. F.; Tang, R. M. Y.; Barardo, D.; Halliwell, B.; Moore, P. K.; Gruber, J. Lifespan and Healthspan Benefits of Exogenous H2S in C. Elegans Are Independent from Effects Downstream of Eat-2 Mutation. *npj Aging Mech. Dis.* **2020**, *6*, 6.
(36) Qabazard, B.; Li, L.; Gruber, J.; Peh, M. T.; Ng, L. F.; Kumar, S. D.; Rose, P.; Tan, C. H.; Dymock, B. W.; Wei, F.; Swain, S. C.; Halliwell, B.; Stürzenbaum, S. R.; Moore, P. K. Hydrogen Sulfide Is an Endogenous Regulator of Aging in Caenorhabditis Elegans. *Antioxid. Redox Signal.* **2014**, *20*, 2621−2630.
(37) Qabazard, B.; Ahmed, S.; Li, N.; Arlt, V. M.; Moore, P. K.; Stürzenbaum, S. R. C. Elegans Aging Is Modulated by Hydrogen Sulfide and the Sulfhydrylase/Cysteine Synthase Cysl-2. *PLoS One* **2013**, *8*, No. e80135.
(38) Ellwood, R. A.; Hewitt, J. E.; Torregrossa, R.; Philp, A. M.; Hardee, J. P.; Hughes, S.; van de Klashorst, D.; Gharahdaghi, N.; Anupom, T.; Slade, L.; Deane, C. S.; Cooke, M.; Etheridge, T.; Piasecki, M.; Antebi, A.; Lynch, G. S.; Philp, A.; Vanapalli, S. A.; Whiteman, M.; Szewczyk, N. J. Mitochondrial Hydrogen Sulfide Supplementation Improves Health in the C. Elegans Duchenne Muscular Dystrophy Model. *Proc. Natl. Acad. Sci. U.S.A.* **2021**, *118*, No. e2018342118.
(39) Dulac, M.; Nagarathinam, C.; Dansette, P.; Mansuy, D.; Boucher, J. L. Mechanism of H2S Formation from the Metabolism of Anetholedithiolethione and Anetholedithiolone by Rat Liver Microsomes. *Drug Metab. Dispos.* **2019**, *47*, 1061−1065.
(40) Harlow, P. H.; Perry, S. J.; Widdison, S.; Daniels, S.; Bondo, E.; Lamberth, C.; Currie, R. A.; Flemming, A. J. The Nematode Caenorhabditis Elegans as a Tool to Predict Chemical Activity on Mammalian Development and Identify Mechanisms Influencing Toxicological Outcome. *Sci. Rep.* **2016**, *6*, No. 22965.
(41) Diez, V.; Traikov, S.; Schmeisser, K.; Adhikari, A. K.; Kurzchalia, T. V. Glycolate Combats Massive Oxidative Stress by Restoring Redox Potential in Caenorhabditis Elegans. *Commun. Biol.* **2021**, *4*, 151.
(42) Chen, B.; Li, W.; Lv, C.; Zhao, M.; Jin, H.; Jin, H.; Du, J.; Zhang, L.; Tang, X. Fluorescent Probe for Highly Selective and Sensitive Detection of Hydrogen Sulfide in Living Cells and Cardiac Tissues. *Analyst* **2013**, *138*, 946−951.
(43) Ionescu-Tucker, A.; Cotman, C. W. Emerging Roles of Oxidative Stress in Brain Aging and Alzheimer's Disease. *Neurobiol. Aging* **2021**, *107*, 86−95.
(44) Di Domenico, F.; Pupo, G.; Giraldo, E.; Badìa, M. C.; Monllor, P.; Lloret, A.; Eugenia Schininà, M.; Giorgi, A.; Cini, C.; Tramutola, A.; Butterfield, D. A.; Viña, J.; Perluigi, M. Oxidative Signature of Cerebrospinal Fluid from Mild Cognitive Impairment and Alzheimer Disease Patients. *Free Radical Biol. Med.* **2016**, *91*, 1−9.
(45) Hensley, K.; Hall, N.; Subramaniam, R.; Cole, P.; Harris, M.; Aksenov, M.; Aksenova, M.; Gabbita, S. P.; Wu, J. F.; Carney, J. M.; Lovell, M.; Markesbery, W. R.; Butterfield, D. A. Brain Regional Correspondence Between Alzheimer's Disease Histopathology and Biomarkers of Protein Oxidation. *J. Neurochem.* **2002**, *65*, 2146−2156.
(46) Butterfield, D. A.; Castegna, A.; Lauderback, C. M.; Drake, J. Evidence That Amyloid Beta-Peptide-Induced Lipid Peroxidation and Its Sequelae in Alzheimer's Disease Brain Contribute to Neuronal Death. *Neurobiol. Aging* **2002**, *23*, 655−664.
(47) Selley, M. L.; Close, D. R.; Stern, S. E. The Effect of Increased Concentrations of Homocysteine on the Concentration of (E)-4-Hydroxy-2-Nonenal in the Plasma and Cerebrospinal Fluid of Patients with Alzheimer's Disease. *Neurobiol. Aging* **2002**, *23*, 383−388.
(48) Shanbhag, N. M.; Evans, M. D.; Mao, W.; Nana, A. L.; Seeley, W. W.; Adame, A.; Rissman, R. A.; Masliah, E.; Mucke, L. Early Neuronal Accumulation of DNA Double Strand Breaks in Alzheimer's Disease. *Acta Neuropathol. Commun.* **2019**, *7*, 77.
(49) Singh, A.; Kukreti, R.; Saso, L.; Kukreti, S. Oxidative Stress: A Key Modulator in Neurodegenerative Diseases. *Molecules* **2019**, *24*, 1583.
(50) Alexander, A. G.; Marfil, V.; Li, C. Use of C. Elegans as a Model to Study Alzheimer's Disease and Other Neurodegenerative Diseases. *Front. Genet.* **2014**, *5*, 279.
(51) Yoon, D. S.; Lee, M.-H.; Cha, D. S. Measurement of Intracellular ROS in Caenorhabditis Elegans Using 2′,7′-Dichlorodihydrofluorescein Diacetate. *Bio-Protocols* **2018**, *8*, No. e2774.
(52) Moreno-García, A.; Kun, A.; Calero, O.; Medina, M.; Calero, M. An Overview of the Role of Lipofuscin in Age-Related Neurodegeneration. *Front. Neurosci.* **2018**, *12*, 464.
(53) Caito, S. W.; Aschner, M. Quantification of Glutathione in Caenorhabditis Elegans. *Curr. Protoc. Toxicol.* **2015**, *64*, 6.18.1−6.18.6.
(54) Karran, E.; Mercken, M.; Strooper, B. De. The Amyloid Cascade Hypothesis for Alzheimer's Disease: An Appraisal for the Development of Therapeutics. *Nat. Rev. Drug Discovery* **2011**, *10*, 698−712.
(55) Kim, H. Y.; Kim, H. V.; Jo, S.; Lee, C. J.; Choi, S. Y.; Kim, D. J.; Kim, Y. EPPS Rescues Hippocampus-Dependent Cognitive Deficits in APP/PS1 Mice by Disaggregation of Amyloid-Beta Oligomers and Plaques. *Nat. Commun.* **2015**, *6*, No. 8997.
(56) Rajasekhar, K.; Chakrabarti, M.; Govindaraju, T. Function and Toxicity of Amyloid Beta and Recent Therapeutic Interventions Targeting Amyloid Beta in Alzheimer's Disease. *Chem. Commun.* **2015**, *51*, 13434−13450.
(57) Sevigny, J.; Chiao, P.; Bussière, T.; Weinreb, P. H.; Williams, L.; Maier, M.; Dunstan, R.; Salloway, S.; Chen, T.; Ling, Y.; O'Gorman, J.; Qian, F.; Arastu, M.; Li, M.; Chollate, S.; Brennan, M. S.; Quintero-Monzon, O.; Scannevin, R. H.; Arnold, H. M.; Engber, T.; Rhodes, K.; Ferrero, J.; Hang, Y.; Mikulskis, A.; Grimm, J.; Hock, C.; Nitsch, R. M.; Sandrock, A. The Antibody Aducanumab Reduces Aβ Plaques in Alzheimer's Disease. *Nature* **2016**, *537*, 50−56.
(58) Link, C. D. Expression of Human β-Amyloid Peptide in Transgenic Caenorhabditis Elegans. *Proc. Natl. Acad. Sci. U.S.A.* **1995**, *92*, 9368−9372.
(59) Tangrodchanapong, T.; Sobhon, P.; Meemon, K. Frondoside A Attenuates Amyloid-β Proteotoxicity in Transgenic Caenorhabditis Elegans by Suppressing Its Formation. *Front. Pharmacol.* **2020**, *11*, No. 553579.

https://doi.org/10.1021/acschemneuro.2c00402
ACS Chem. Neurosci. XXXX, XXX, XXX−XXX

(60) Sashidhara, K. V.; Modukuri, R. K.; Jadiya, P.; Dodda, R. P.; Kumar, M.; Sridhar, B.; Kumar, V.; Haque, R.; Siddiqi, M. I.; Nazir, A. Benzofuran-Chalcone Hybrids as Potential Multifunctional Agents against Alzheimer's Disease: Synthesis and in Vivo Studies with Transgenic Caenorhabditis Elegans. *ChemMedChem* **2014**, *9*, 2671−2684.
(61) H. Ferreira-Vieira, T.; M. Guimaraes, I.; R. Silva, F.; M. Ribeiro, F. Alzheimer's Disease: Targeting the Cholinergic System. *Curr. Neuropharmacol.* **2016**, *14*, 101−115.
(62) Haque, R.; Nazir, A. SMAD Transcription Factor, Sma-9, Attunes TGF-β Signaling Cascade Towards Modulating Amyloid Beta Aggregation and Associated Outcome in Transgenic C. Elegans. *Mol. Neurobiol.* **2016**, *53*, 109−119.
(63) Mattson, M. P.; Pedersen, W. A. Effects of Amyloid Precursor Protein Derivatives and Oxidative Stress on Basal Forebrain Cholinergic Systems in Alzheimer's Disease. *Int. J. Dev. Neurosci.* **1998**, *16*, 737−753.
(64) Kar, S.; Issa, A. M.; Seto, D.; Auld, D. S.; Collier, B.; Quirion, R. Amyloid β-Peptide Inhibits High-Affinity Choline Uptake and Acetylcholine Release in Rat Hippocampal Slices. *J. Neurochem.* **2002**, *70*, 2179−2187.
(65) Auld, D. S.; Kar, S.; Quirion, R. β-Amyloid Peptides as Direct Cholinergic Neuromodulators: A Missing Link? *Trends Neurosci.* **1998**, *21*, 43−49.
(66) Schliebs, R.; Arendt, T. The Cholinergic System in Aging and Neuronal Degeneration. *Behav. Brain Res.* **2011**, *221*, 555−563.
(67) Thorson, M. K.; Majtan, T.; Kraus, J. P.; Barrios, A. M. Identification of Cystathionine β-Synthase Inhibitors Using a Hydrogen Sulfide Selective Probe. *Angew. Chem., Int. Ed.* **2013**, *52*, 4641−4644.
(68) Sashidhara, K. V.; Modukuri, R. K.; Jadiya, P.; Dodda, R. P.; Kumar, M.; Sridhar, B.; Kumar, V.; Haque, R.; Siddiqi, M. I.; Nazir, A. Benzofuran−Chalcone Hybrids as Potential Multifunctional Agents against Alzheimer's Disease: Synthesis and in Vivo Studies with Transgenic Caenorhabditis Elegans. *ChemMedChem* **2014**, *9*, 2671−2684.
(69) Zhang, Y.; Tingley, F. D.; Tseng, E.; Tella, M.; Yang, X.; Groeber, E.; Liu, J.; Li, W.; Schmidt, C. J.; Steenwyk, R. Development and Validation of a Sample Stabilization Strategy and a UPLC-MS/MS Method for the Simultaneous Quantitation of Acetylcholine (ACh), Histamine (HA), and Its Metabolites in Rat Cerebrospinal Fluid (CSF). *J. Chromatogr. B* **2011**, *879*, 2023−2033.

https://doi.org/10.1021/acschemneuro.2c00402
ACS Chem. Neurosci. XXXX, XXX, XXX−XXX